Tuning of polarization-dependent whispering gallery modes in grapefruit microstructured optical fibers infiltrated with negative dielectric anisotropy liquid crystals

Chengkun Yang, Hao Zhang, Bo Liu, Haifeng Liu, Chao Wang and Shiwei Lin

***Abstract*—An electrically tunable whispering gallery mode (WGM) microresonator based on microstructured optical fibers (MOFs) infiltrated with negative dielectric anisotropy liquid crystals (LCs) is proposed and experimentally demonstrated. Experimental results indicate that the second radial order mode of the MOF microresonator has stronger electric field response than the first radial order mode and the resonance dip for TE polarization mode is more sensitive to the applied electric field intensity in comparison with the TM polarization mode resonance dip. The Freedericksz transition threshold of the proposed MOF microresonator is experimentally found to be about 2.0 $\mathrm{V\mu m^{-1}}$. The electrically tunable microresonator integrated with negative dielectric anisotropy LCs is anticipated to find potential applications in optical filtering, all-optical switching, and electrically controlled micro-optics devices.**

***Index Terms*—Whispering gallery mode, Optical microresonator, Microstructured optical fiber, Liquid crystals, Mode tuning.**

I. Introduction

Owing to their desirable merits, including high optical quality, enhanced optical field, and small mode volume, optical whispering gallery mode (WGM) microresonators have attracted growing research interest in various fundamental as well as applied research areas. In WGM microresonators, light is trapped and confined inside the optical waveguides with circular symmetry due to the total internal reflection occurring at the interface between high- and low-index media. Microfluidic optical resonators have the unique properties of liquids to provide novel platforms for sensing [1, 2], low threshold lasers [3, 4], biochemical analysis and detection applications [5-7], and they have become the research subjects of related studies in the field of nonlinear optics [8] and optomechanics [9, 10]. Tuning of WGMs in microresonators have been an interesting research topic since the pioneering studies on WGM devices in the 1990s. As reported in previous studies, tunable WGM microresonators could be achieved by altering microresonator size [11, 12], controlling environmental temperature [13, 14], changing solution concentration or simply replacing one fluid infiltrated in the microresonator with another[4]. Although large WGM resonance wavelength shift could be achieved, it would be difficult to precisely control the microresonator size and environmental temperature. And moreover, the wavelength shift range is rather limited by changing the solution concentration or alternating the type of infiltrated liquids. The above disadvantages make WGM tuning rather slow, inaccurate, and impractical for practical applications. Electrical tuning approach could be employed to realize precise control and fast modulation of WGMs, however, design of electrically tuned microring resonators is still a quite challenging issue [15, 16]. Studies on optical microresonators based on liquid crystals (LCs) [17, 18] provide promising WGM tuning schemes through controlling the applied electric field intensity or changing environmental temperature to achieve large wavelength shifts. However, due to the susceptibility of PDMS coating serving as the LC chamber, the microcavity shape is apt to experience irregular changes when strong electric field is applied, which deteriorates the performances of WGM devices to some extent. In order to solve this issue, we recently proposed an electrically tuned microstructured optical fiber (MOF) infiltrated with positive dielectric anisotropy LCs [19], where only the WGM resonance wavelength corresponding to TM polarization mode was experimentally acquired and tuned by changing the applied electric field intensity.

A good variety of tunable optical devices based on photonic crystal fibers (PCFs) infiltrated with negative dielectric anisotropy liquid crystals have been reported in the past few years [20-22]. In this paper, we report an electrically tuned

Manuscript received April 10, 2018. This work was jointly supported by the National Natural Science Foundation of China under Grant Nos. 11774181, 61727815, 11274182, 61377095 and 11004110, Science & Technology Support Project of Tianjin under Grant No. 16YFZCSF00400, and the 863 National High Technology Program of China under Grant No. 2013AA014201. (Corresponding authors: Hao Zhang and Bo Liu)

C. Yang, H. Zhang, B. Liu, H. Liu, and S. Lin are with Tianjin Key Laboratory of Optoelectronic Sensor and Sensing Network Technology, Institute of Modern Optics, Nankai University, Tianjin 300350, China. (e-mail: yangchk1225@163.com,haozhang@nankai.edu.cn,liubo@nankai.edu.cn, hfliu@mail.nankai.edu.cn, 477623614@qq.com) C. Wang is with School of Engineering and Digital Arts, University of Kent, Canterbury CT2 7NT, United Kingdom. (e-mail: c.wang@kent.ac.uk)

MOF microresonator infiltrated with negative dielectric anisotropy liquid crystals. A segment of grapefruit MOF serves as the cylindrical microresonator where the WGMs are excited by evanescent coupling of the light propagating through a thin fiber taper placed in perpendicular contact with the MOF microresonator. We use the MOF-based microresonator to investigate the tunability of the TE- and TM-polarized as well as different radial order WGMs. The proposed MOF-based microresonator has several advantages such as ease of manipulation, fast response, and good spectral reversibility, which ensure its potential applications as highly integrated tunable WGM devices.

II. Experimental Setup And Operation Principle

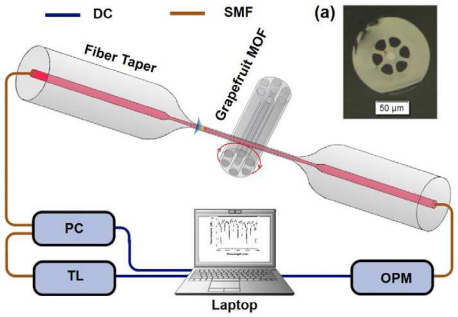

Fig. 1. Schematic diagram of the performance test system for the proposed MOF-based microresonator integrated with negative negative dielectric anisotropy LCs. TL, tunable laser; PC, polarization controller; OPM, optical power meter; DC, data cable; SMF, single-mode fiber; grapefruit MOF, grapefruit microstructred optical fiber. Insert (a) gives a cross-sectional microscopic image of the grapefruit MOF.

Fig.1 illustrates the experimental setup for the proposed MOF-based WGM microresonator infiltrated with negative dielectric anisotropy LCs. A tunable laser (PC, N7786B produced by Keysight Technologies, US) with a wavelength range of 1520 nm ~1560 nm is coupled to a polarization controller (PC, N7786B produced by Keysight Technologies, US) which in turn is coupled to the input end of tapered fiber, the output of which is coupled to an optical power meter (OPM, N7744A produced by Keysight Technologies, US). The spectral information is transferred to a laptop for data processing.

In our experiment, a segment of grapefruit MOF has one rings of air holes of 15 μm in diameter surrounding its solid core. Negative dielectric anisotropy LCs (BHR28000-100, Bayi Space LCD, China) is infiltrated into the grapefruit MOF by dipping one end of the fiber into the LCs so that the liquids would flow into the air-hole channels in the presence of capillary forces. The negative dielectric anisotropy LCs have the ordinary and extraordinary refractive indices of $n_0 = 1.485$ and $n_e = 1.575$ around 589.3 nm at 20 ℃. The electrical permittivity at 1 kHz is $\varepsilon_\perp = 17.9$ in the ordinary axis and $\varepsilon_{//} = 6.3$ in the extraordinary axis at 20 ℃, resulting in a dielectric anisotropy of $\Delta\varepsilon$ =-11.6. Since WGMs are normally propagating close to the outer periphery of the circular optical waveguide, in order to enhance the WGM resonance wavelength sensitivity to the refractive index variation of the LCs kept inside the air holes, the silica background of the grapefruit MOF is partially etched by using hydrofluoric acid at a concentration of 40% by weight. The diameter of the MOFs infiltrated with LCs after HF etching processing is about 63.36 μm and the gap between the holes and the outer surface is about 1.68 μm.

III. Experimental Results And Discussion

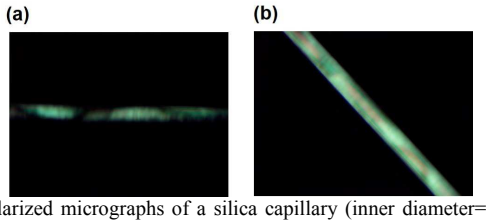

Fig. 2. Polarized micrographs of a silica capillary (inner diameter= 30 μm) infiltrated with negative dielectric anisotropy liquid crystals. Capillary is angled at 0 degrees (a) and 45 degrees (b) with respect to the polarizer axis.

WGMs in optical microcavities could be generally classified into two different polarization components, namely the TE mode and the TM mode whose electric field respectively oscillates parallel to or perpendicular to the outer surface of the microresonator. Depending on the mesophase and surface boundary conditions, the LC mesogens typically turn out a specific alignment with minimized free energy. By using a polarized microscopy, we found that negative dielectric anisotropy LCs infiltrated in a 30 μm fused silica capillary tube was aligned in a planar alignment where the LCs are mainly

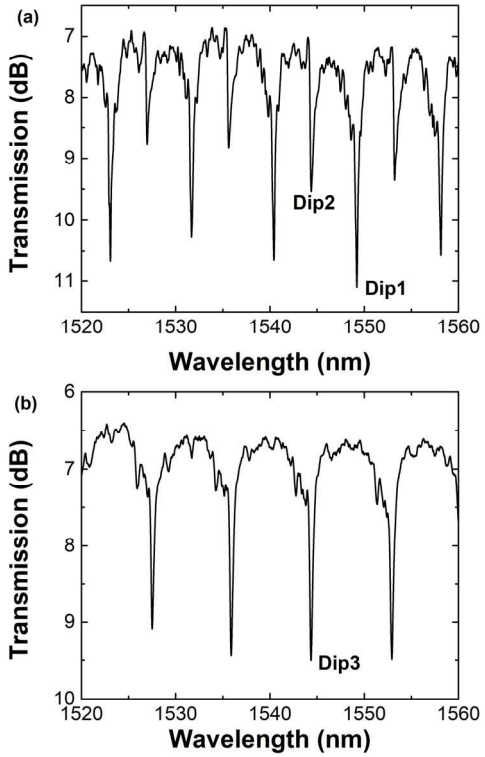

Fig. 3. Experimentally acquired WGM transmission spectra for the MOF microresonator infiltrated with negative dielectric anisotropy LCs: (a) TM polarization mode; (b) TE polarization mode.

orientated along the fiber axis [23], as shown in Fig. 2. In silica capillaries, the LC molecular director tends to align in the fiber axis, and thus TM-polarized light is exposed to the ordinary refractive index (no) of the LC molecules while the TE-polarized light experiences the extraordinary refractive index (ne).

By adjusting the polarization state of the incident light, WGM resonance dips could be obtained in the transmission spectrum, as shown in Fig. 3. Due to its better WGM purity, the MOF microresonator with a diameter of 63.36 μm is selected to investigate the WGM properties of the MOF microresonator. It could be seen that the excited WGMs belong to the TM_m^1, TM_M^2 and TE_m^1 categories, and no higher radial order (l > 2) mode is excited.

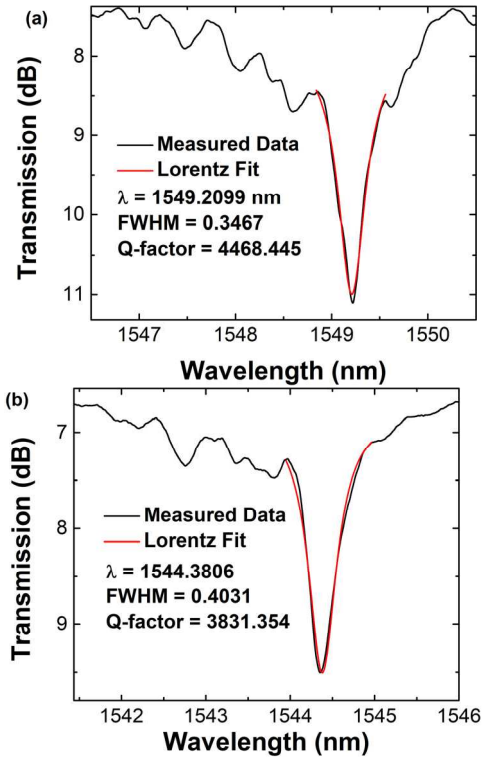

Fig. 4 Lorentzian fit of the WGM transmission spectra with estimated Q-factors for the grapefruit MOF microresonator infiltrated with negative dielectric anisotropy LCs. (a) TM polarization mode for Dip 1; (b) TE polarization mode for Dip 3.

Amongst many parameters that characterize the WGM properties of miroresonators, the quality factor (Q) may be the most important one, which is highly relevant to the lifetime of the light energy reserved in the microcavity. Lorentz fit is performed on the WGM transmission spectra for the resonance Dip1 and Dip3 that respectively correspond to the TM mode and TE polarization mode, as shown in Fig. 4(a) and (b). Q factors of the above resonance dips could be calculated by using $Q = \lambda/\Delta\lambda$, where λ is central resonance wavelength and Δλ is full width half-maximum (FWHM) of the resonance peak. As shown in Fig. 4, when no electric field is applied, the Q-factors for Dip 1 and Dip 3 are respectively 4.47×10^3 and 3.83×10^3, which are in a typical order of magnitude of the cylindrical WGM microresonators filled with LCs. The relatively low Q-factors are mainly determined by strong scattering of LC molecules.

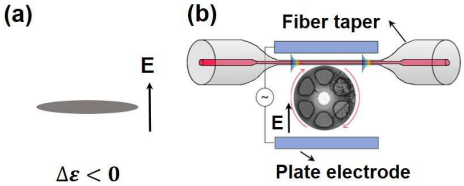

Fig. 5 (a) A negative dielectric anisotropy LC molecule under applied high electric field; (b) Illustration of a grapefruit-MOF-based microresonator under applied AC electric voltage.

Negative dielectric anisotropy liquid crystals with negative dielectric anisotropy($\Delta\varepsilon = \varepsilon_{//} - \varepsilon_{\perp} < 0$) have good thermal and electric tunability whose molecules tend to re-orientate perpendicular to the applied electric field when the electric field intensity is larger than Freedericksz threshold, as shown in Fig. 5 (a). To investigate the electrical tuning characteristics of the proposed MOF-based microresonator infiltrated with negative dielectric anisotropy LCs, a 1kHz AC electric field is applied perpendicular to the axis of symmetry of the microresonator by employing a pair of plate electrodes with a ~200-μm gap between them. Structural deformation of the negative dielectric anisotropy LC molecules kept inside the microresonator is led by the applied electric field to alter the effective refractive index of the WGMs circulating inside the birefringent microresonator, and consequently WGM resonance dips would shift in response to the increment of applied electric field intensity.

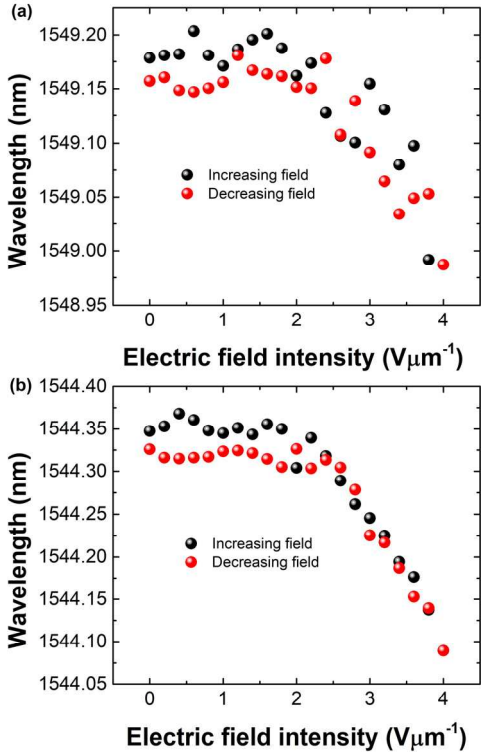

Fig. 6. WGM resonance wavelength for the TM polarization mode as functions of applied electric field intensity. (a) Dip1 for the first-order WGM; (b) Dip 2 for the second-order WGM.

Fig. 6(a) and (b) show WGM resonance wavelength for Dip 1 and Dip 2 that both correspond to the TM polarization mode as functions of applied electric field intensity. From Fig. 6 (a), it could be seen that as the applied electric field is strengthened the WGM resonance dips irregularly shift toward shorter wavelength region. As the applied electric field intensity increases to 4 Vμm^{-1}, Dip1 irregularly shifts by 0.1915 nm. From Fig. 6(b), it can be seen that the second-order WGMresonance dip exhibits a blue shift with the increment of the applied electric field strength. When the applied electric field intensity is less than 2.2 Vμm^{-1}, WGM resonance wavelength turns out irregular fluctuations, which implies that below this particular electric field intensity, thermal motion of the LC molecules plays a dominant role in the WGM characteristics of the proposed microresonator. When the electric field intensity ranges from 2.2 Vμm^{-1} to 4 Vμm^{-1}, the WGM resonance dips regularly move toward shorter wavelength region with the increment of applied electric field intensity. As the applied electric field weakens, the resonance dip moves toward longer wavelength region. The resonance dip shows good spectral reversibility within an electric intensity range of 4 Vμm^{-1} to 2.2 Vμm^{-1}. Below this particular applied electric field strength of 2.2 Vμm^{-1}, the resonance dip would no longer maintain good spectral reversibility. As the applied electric field strength increases to 4 Vμm^{-1}, the WGM resonance dip regularly moves by 0.258 nm.

As shown in Fig. 6, the second radial order mode is more sensitive to the variation of applied electric field intensity in comparison with the first radial order mode. This could be mainly attributed to the fact that the second radial order mode is closer to the liquid core than the first radial mode, and the larger fraction of mode distributed in the liquid core would substantially enhance the interaction between the resonance mode and the liquid sample[24].

From Fig. 7(a), it could be seen that as the applied electric field gets strengthened, the decrease of effective refractive index would cause Dip3 to move toward shorter wavelength region. Fig. 7(b) gives WGM resonance wavelength of Dip 3 as functions of applied electric field intensity for TE polarization mode. From this figure, it could be found that when the applied electric field strength is lower than 2 Vμm^{-1}, WGM resonance dip exhibits irregular fluctuations, which means that below this particular electric filed intensity, thermal motions of LCs molecules play a dominant role in the WGM characteristics. When applied electric field strength ranges from 2 Vμm^{-1} to 4 Vμm^{-1}, the WGM resonance dip linearly shifts toward shorter wavelength region with the increment of the applied electric field intensity and the wavelength sensitivity reaches 0.324 $nm/V\mu m^{-1}$, and the maximum spectral shift is 0.81 nm. Further experimental observation of WGM resonance wavelength shift in response to the decrease of the applied electric field intensity indicates that the wavelength responses of WGM resonance dips have good reversibility.

From Fig. 6 and Fig. 7, it could be also found that the resonance dip corresponding to the TE polarization mode has higher wavelength sensitivity to the applied electric field intensity compared with the one for the TM polarization mode. As negative dielectric anisotropy LCs are in planar alignment, the TM and TE modes would sense the ordinary (no) and extraordinary (ne) refractive indices, respectively. Since the extraordinary (ne) refractive indices is more sensitive to the variation of applied electric field than the ordinary (no) refractive indices, the TE polarization resonance dip shows larger wavelength shift than TM polarization resonance dip. Further experimental observation on the WGM resonance wavelength shift with the decrease of applied electric field intensity shows that both of the resonance dips corresponding to the TE and TM polarization modes have good spectral reversibility.

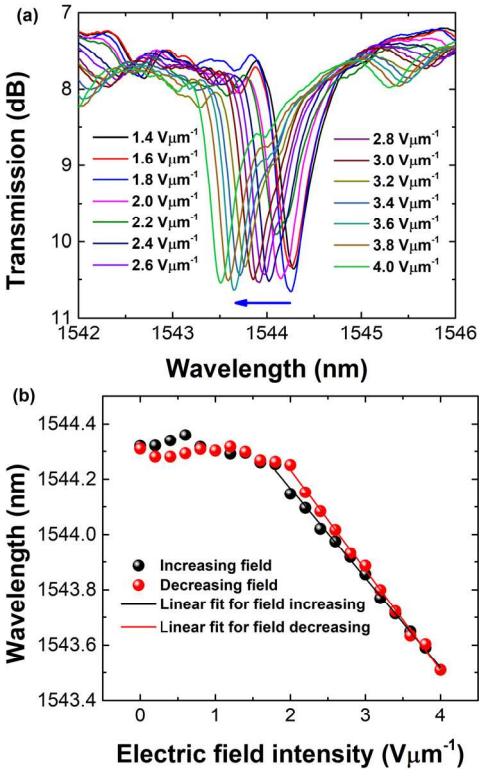

Fig. 7. (a) Transmission spectra of the grapefruit-MOF-based microresonator filled with negative dielectric anisotropy LCs under the different applied electric field intensities for Dip3. Arrows in these figures indicate the spectral shift direction as the applied electric field intensity increases. (b) WGM resonance dip wavelength as functions of applied electric field strength for TE polarization mode.

Besides, the experimental results in Fig. 6 and Fig. 7 indicate that there exist some electrical field intensity threshold above or below which the WGM resonance dips would exhibit reverse wavelength shift behaviors. This interesting phenomenon could be attributed to the Freedericksz transition[25] which is present in most LC devices, where the director reorientation could be easily manipulated by the applied field intensity. If the applied the electric field intensity is below the Freedericksz transition threshold, the LC directors would not be re-oriented. However, when the applied electric field intensity exceeds this threshold, the LC deformation would start to emerge. From Fig. 6 and Fig. 7, it could be seen that the Freedericksz transition threshold of proposed MOF microresonator is about 2 Vμm^{-1}, below which the orientation of negative dielectric anisotropy LCs molecules

maintains unchanged. However, when the applied electric field is beyond this specific threshold, the negative dielectric anisotropy LC molecules tend to be re-oriented perpendicular to the applied electric field with the increment of field intensity, which would alter the effective refractive index of the WGMs and cause the WGM resonance dips to move toward shorter wavelength region. The Freedericksz transition threshold is co-determined by surface anchoring energy, elastic torque, electric-field-induced torque, and viscous torque of liquid crystal devices. Therefore, investigation of the Freedericksz transition threshold would be of great significance for the design of low-threshold electrically controlled micro-optics devices

IV. Conclusion

In conclusion, we have proposed and experimentally demonstrated an electrically controlled WGM tuning scheme by employing a grapefruit-MOF-based microresonator integrated with negative dielectric anisotropy LCs. For the TM polarization mode, the resonance dip wavelength corresponding to the second radial order WGM shows higher sensitivity to the applied electric field intensity compared with its first radial order counterpart. For the TE polarization mode, the WGM resonance dip wavelength tuning sensitivity reaches 0.324 $nm/V\mu m^{-1}$ and the maximum spectral shift is up to 0.81 nm. The WGM resonance dip also shows good spectral reversible electric-field-dependent shift behavior. Owing to its high electric field sensitivity and good electric-field-dependent wavelength shift reversibility, this microresonator could be applied for the measurement of electric field strength. Experimental results indicate that the TE polarization resonance dip exhibits stronger responses to the variation of applied electric field in comparison with the TM polarization resonance dip. Freedericksz transition threshold of the proposed MOF microresonator is experimentally found to be about 2 $V\mu m^{-1}$. The disparate resonance wavelength shift behaviors above and below the Frederick transition threshold make the electrically tunable microresonator a good platform to investigate this particular feature of LC materials, which would be of significance for LC sciences and related applications. And moreover, the proposed electrically tunable microresonator integrated with negative dielectric anisotropy LCs is also anticipated to find potential applications in optical filtering, all-optical switching, and electrically controlled micro-optics devices.

V. ACKNOWLWGEMENT

The authors would like to thank Ms. Lirong Zhu from Key Laboratory of Functional Polymer Materials (Nankai University), Ministry of Education, for her assistance in the LC alignment imaging using polarized microscope.

References

[1] C. T. Wang, et al. Highly sensitive optical temperature sensor based on a SiN micro-ring resonator with liquid crystal cladding. Opt Express, 2016, 24, 1002-7.

[2] A. Mahmood, et al. Magnetic field sensing using whispering-gallery modes in a cylindrical microresonator infiltrated with ferronematic liquid crystal. Opt Express, 2017, 25, 12195-202.

[3] S. M. Spillane, T. J. Kippenberg, K. J. Vahala. Ultralow-threshold Raman laser using a spherical dielectric microcavity. Nature, 2002, 415, 621-3.

[4] W. Lee, H. Li, J. D. Suter, K. Reddy, Y. Sun, X. Fan. Tunable single mode lasing from an on-chip optofluidic ring resonator laser. Applied Physics Letters, 2011, 98, 061103.

[5] A. M. Armani, R. P. Kulkarni, S. E. Fraser, R. C. Flagan, K. J. Vahala. Label-free, single-molecule detection with optical microcavities. Science, 2007, 317, 783-7.

[6] M. Li, X. Wu, L. Liu, X. Fan, L. Xu. Self-referencing optofluidic ring resonator sensor for highly sensitive biomolecular detection. Anal Chem, 2013, 85, 9328-32.

[7] T. Ma, et al. Highly Sensitive Biochemical Sensor Based on Two-Layer Dielectric Loaded Plasmonic Microring Resonator. Plasmonics, 2016.

[8] V. S. Ilchenko, A. A. Savchenkov, A. B. Matsko, L. Maleki. Nonlinear optics and crystalline whispering gallery mode cavities. Phys Rev Lett, 2004, 92, 043903.

[9] C. Dong, V. Fiore, M. C. Kuzyk, H. Wang. Transient optomechanically induced transparency in a silica microsphere. Physical Review A, 2013, 87.

[10] C. Dong, V. Fiore, M. C. Kuzyk, H. Wang. Optomechanical dark mode. Science, 2012, 338, 1609-13.

[11] A. Kiraz, A. Kurt, M. A. Dündar, A. L. Demirel. Simple largely tunable optical microcavity. Applied Physics Letters, 2006, 89.

[12] V. D. Ta, R. Chen, H. D. Sun. Tuning whispering gallery mode lasing from self-assembled polymer droplets. Sci Rep, 2013, 3, 1362.

[13] V. R. Anand, S. Mathew, B. Samuel, P. Radhakrishnan, M. Kailasnath. Thermo-optic tuning of whispering gallery mode lasing from a dye-doped hollow polymer optical fiber. Opt Lett, 2017, 42, 2926-9.

[14] Z. Liu, et al. Whispering gallery mode temperature sensor of liquid microresonastor. Optics Letters, 2016, 41, 4649.

[15] T. J. Wang, C. H. Chu, C. Y. Lin. Electro-optically tunable microring resonators on lithium niobate. Opt Lett, 2007, 32, 2777-9.

[16] B. Maune, R. Lawson, C. Gunn, A. Scherer, L. Dalton. Electrically tunable ring resonators incorporating nematic liquid crystals as cladding layers. Applied Physics Letters, 2003, 83, 4689-91.

[17] T. A. Kumar, M. A. Mohiddon, N. Dutta, N. K. Viswanathan, S. Dhara. Detection of phase transitions from the study of whispering gallery mode resonance in liquid crystal droplets. Applied Physics Letters, 2015, 106, 051101.

[18] M. Humar, M. Ravnik, S. Pajk, I. Muševič. Electrically tunable liquid crystal optical microresonators. Nature Photonics, 2009, 3, 595-600.

[19] C. Yang, H. Zhang, B. Liu, S. lin, Y. Li, H. Liu. Electrically tunable whispering gallery mode microresonator based on a grapefruit-microstructured optical fiber infiltrated with nematic liquid crystals. Optics Letters, 2017, 42.

[20] L. Wei, L. Eskildsen, J. Weirich, L. Scolari, T. T. Alkeskjold, A. Bjarklev. Continuously tunable all-in-fiber devices based on thermal and electrical control of negative dielectric anisotropy liquid crystal photonic bandgap fibers. Appl Opt, 2009, 48, 497-503.

[21] L. Wei, T. T. Alkeskjold, A. Bjarklev. Electrically tunable bandpass filter using solid-core photonic crystal fibers filled with multiple liquid crystals. Optics Letters, 2010, 35, 1608-10.

[22] A. M. Stolyarov, L. Wei, F. Sorin, G. Lestoquoy, J. D. Joannopoulos, Y. Fink. Fabrication and characterization of fibers with built-in liquid crystal channels and electrodes for transverse incident-light modulation. Applied Physics Letters, 2012, 101.

[23] T. Alkeskjold, et al. All-optical modulation in dye-doped nematic liquid crystal photonic bandgap fibers. Opt Express, 2004, 12, 5857-71.

[24] H. Li, X. D. Fan. Characterization of sensing capability of optofluidic ring resonator biosensors. Applied Physics Letters, 2010, 97.

[25] V. Zolina. Forces causing the orientation of an anisotropic liquid. Trans Faraday Soc, 1933, 29, 919-30.

Chengkun Yang received the bachelor degree in Applied Physics from Tianjin Polytechnic University, China, in 2014, and is currently a Ph.D. candidate in Optics in the Institute of Modern Optics, Nankai University. His research interests

focuses on microstructured-fiber-based tunable whispering gallery mode devices integrated with functional materials.

Hao Zhang received the Ph.D. degree in Optics from Nankai University, China, in 2005. He is currently a professor in the Institute of Modern Optics, Nankai University. His research interests include micro/nanostructured fiber devices, novel fiber sensors, and fiber lasers.

Bo Liu received the Ph.D. degree in Optics from Nankai University, Tianjin, China, in 2004. He is currently a professor in the Institute of Modern Optics, Nankai University. His major research interests include fiber sensors, fiber-grating-based photonic devices, and interrogation systems.

Haifeng Liu received the Ph.D. degree in Optics from Nankai University, China, in 2016. He is currently an Engineering in the Institute of Modern Optics, Nankai University. His research interests include novel fiber-optic devices based on functional materials and their applications.

Chao Wang received the Ph. D. degree in Electrical and Computer Engineering from University of Ottawa, Canada, in 2011. He is currently a Senior Lecturer in the School of Engineering and Digital Arts, University of Kent, UK. His research interests lie in inter-disciplinary areas that study the interaction between Photonics and other traditional or state-of-the-art technologies in different fields, such as microwave photonics, optical communications, and biophotonics for widespread industrial, communications, biomedical and defense applications.

Shiwei Lin received the bachelor degree in Optoelectronic Technology and Science from Nankai University, China, in 2015, and is currently a M.S. candidate in Optics in the Institute of Modern Optics, Nankai University. His research interests focuses on novel fiber-optic devices, smart fiber structures, and their applications in the field optical sensing technology.